Liouville Quantum Gravity as a Mating of Trees

Bertrand Duplantier, Jason Miller, and Scott Sheffield

CEA/Saclay and Massachusetts Institute of Technology

September 30, 2014

Overview

Part I: Gluing a pair of CRTs

Part II: Scaling limits of random planar maps and Liouville quantum gravity

Part III: Results

Part I: Gluing a pair of CRTs

Gluing a pair of CRTs

X, Y independent Brownian excursions on $[0,1]$. Pick $C > 0$ large so that the graphs of X and $C - Y$ are disjoint.

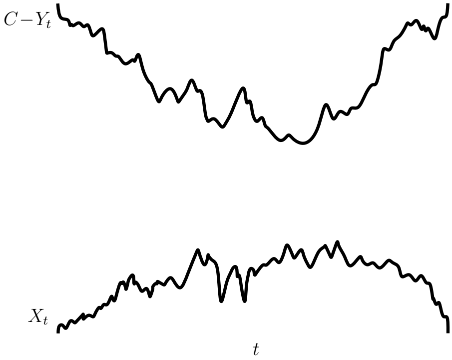

Gluing a pair of CRTs

X, Y independent Brownian excursions on $[0,1]$. Pick $C > 0$ large so that the graphs of X and $C - Y$ are disjoint.

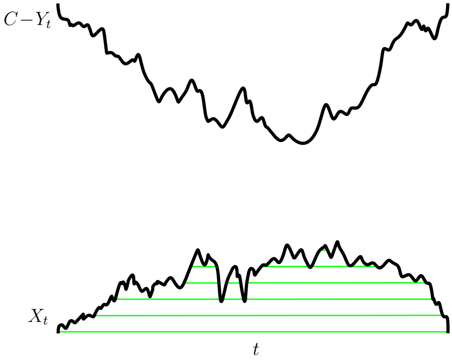

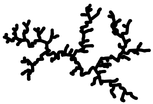

- Identify points on the graph of X if they are connected by a **horizontal** line which is below the graph; yields a continuum random tree (CRT)

Gluing a pair of CRTs

X, Y independent Brownian excursions on $[0,1]$. Pick $C > 0$ large so that the graphs of X and $C - Y$ are disjoint.

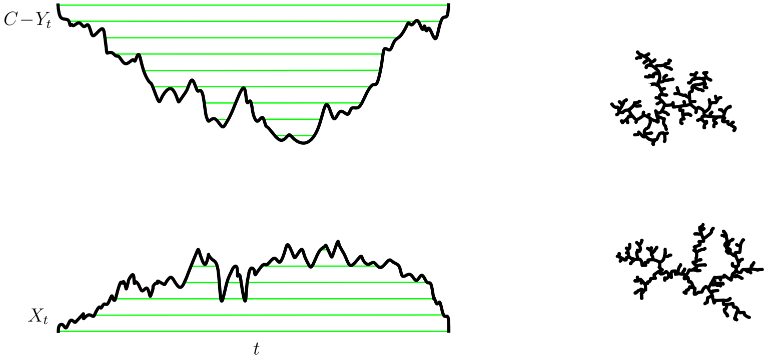

- Identify points on the graph of X if they are connected by a **horizontal** line which is below the graph; yields a continuum random tree (CRT)
- Same for $C - Y_t$ yields an independent CRT

Gluing a pair of CRTs

X, Y independent Brownian excursions on $[0,1]$. Pick $C > 0$ large so that the graphs of X and $C - Y$ are disjoint.

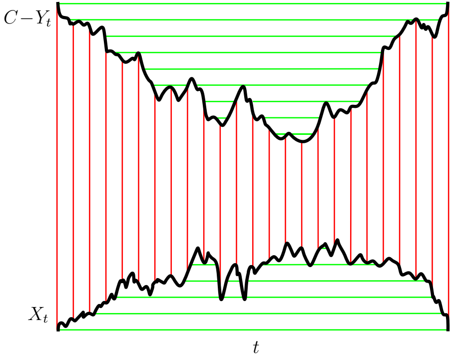

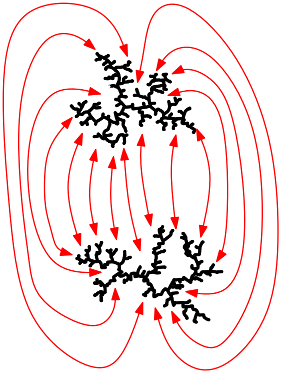

- Identify points on the graph of X if they are connected by a **horizontal** line which is below the graph; yields a continuum random tree (CRT)
- Same for $C - Y_t$ yields an independent CRT
- Glue the CRTs together by declaring points on the **vertical** lines to be equivalent

Gluing a pair of CRTs

X, Y independent Brownian excursions on $[0,1]$. Pick $C > 0$ large so that the graphs of X and $C - Y$ are disjoint.

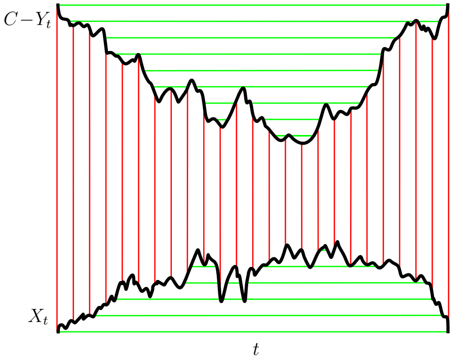

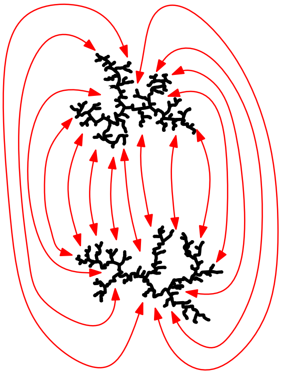

- Identify points on the graph of X if they are connected by a **horizontal** line which is below the graph; yields a continuum random tree (CRT)
- Same for $C - Y_t$ yields an independent CRT
- Glue the CRTs together by declaring points on the **vertical** lines to be equivalent

Q: What is the resulting structure?

Gluing a pair of CRTs

X, Y independent Brownian excursions on $[0,1]$. Pick $C > 0$ large so that the graphs of X and $C - Y$ are disjoint.

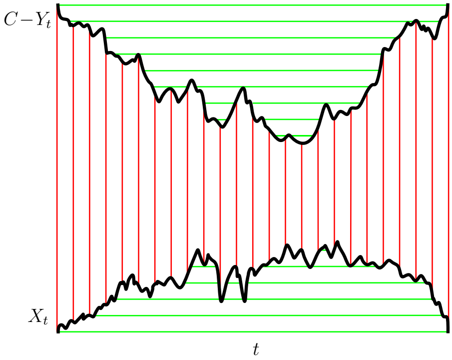

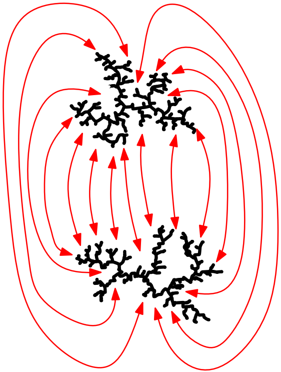

- Identify points on the graph of X if they are connected by a **horizontal** line which is below the graph; yields a continuum random tree (CRT)
- Same for $C - Y_t$ yields an independent CRT
- Glue the CRTs together by declaring points on the **vertical** lines to be equivalent

Q: What is the resulting structure? **A:** Sphere with a space-filling path.

Gluing a pair of CRTs

X, Y independent Brownian excursions on $[0,1]$. Pick $C > 0$ large so that the graphs of X and $C - Y$ are disjoint.

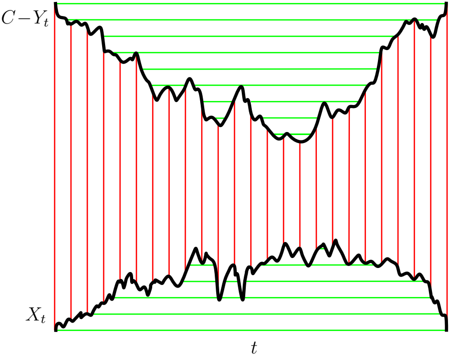

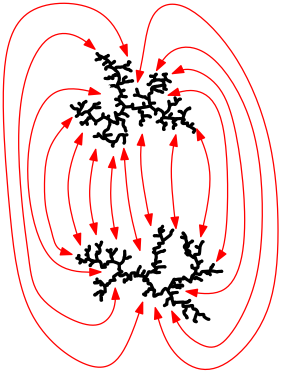

- Identify points on the graph of X if they are connected by a **horizontal** line which is below the graph; yields a continuum random tree (CRT)
- Same for $C - Y_t$ yields an independent CRT
- Glue the CRTs together by declaring points on the **vertical** lines to be equivalent

Q: What is the resulting structure? **A:** Sphere with a space-filling path. A **peanosphere**.

How to check this?

Theorem (Moore 1925)

Let $\cong$ be any topologically closed equivalence relation on the sphere $\mathbf{S}^2$. Assume that each equivalence class is connected and not equal to all of $\mathbf{S}^2$. Then the quotient space $\mathbf{S}^2/\cong$ is homeomorphic to $\mathbf{S}^2$ if and only if no equivalence class separates the sphere into two or more connected components.

- An equivalence relation is topologically closed iff for any two sequences (x_n) and (y_n) with
  - $x_n \cong y_n$ for all n
  - $x_n \to x$ and $y_n \to y$
- we have that $x \cong y$.

Constructing a sphere from a pair of trees

- X, Y ind. Brownian excursions on $[0, 1]$
- **Red**/**green** lines give an $\cong$-relation on $\mathbf{S}^2$

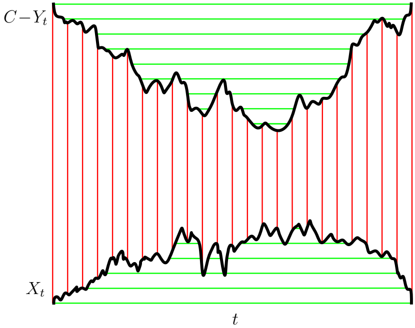

Constructing a sphere from a pair of trees

- X, Y ind. Brownian excursions on $[0, 1]$
- **Red**/**green** lines give an $\cong$-relation on $\mathbf{S}^2$
- Types of equivalence classes:

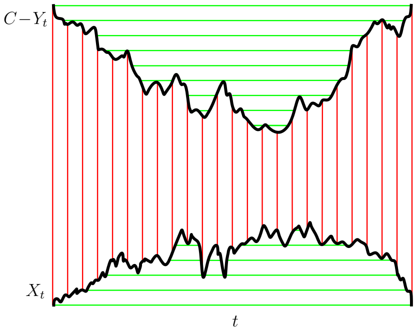

Constructing a sphere from a pair of trees

- X, Y ind. Brownian excursions on $[0, 1]$
- **Red**/**green** lines give an $\cong$-relation on $\mathbf{S}^2$
- Types of equivalence classes:
  1. Outer boundary of rectangle

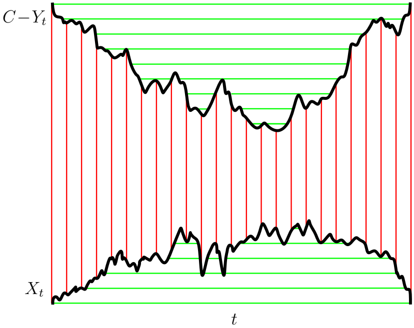

Constructing a sphere from a pair of trees

- X, Y ind. Brownian excursions on $[0, 1]$
- **Red**/**green** lines give an $\cong$-relation on $\mathbf{S}^2$
- Types of equivalence classes:
  1. Outer boundary of rectangle
  2. **V** line which does not share an endpoint with a **H** line

H = horizontal, **V** = vertical

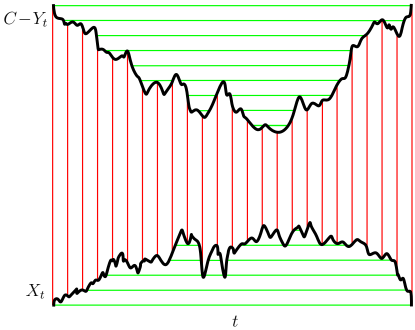

Constructing a sphere from a pair of trees

- X, Y ind. Brownian excursions on $[0, 1]$
- **Red**/**green** lines give an $\cong$-relation on $\mathbf{S}^2$
- Types of equivalence classes:
  1. Outer boundary of rectangle
  2. **V** line which does not share an endpoint with a **H** line
  3. **H** line below X or above $C - Y$ with two **V** lines with common endpoint

H = horizontal, **V** = vertical

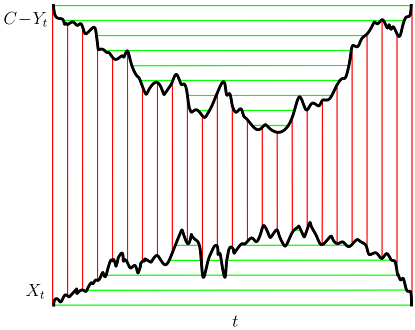

Constructing a sphere from a pair of trees

- X, Y ind. Brownian excursions on $[0, 1]$
- **Red**/**green** lines give an $\cong$-relation on $\mathbf{S}^2$
- Types of equivalence classes:
  1. Outer boundary of rectangle
  2. **V** line which does not share an endpoint with a **H** line
  3. **H** line below X or above $C - Y$ with two **V** lines with common endpoint
  4. **H** line below X or above $C - Y$ with two **V** lines with common endpoint and a third **V** line hitting in the middle

H = horizontal, **V** = vertical

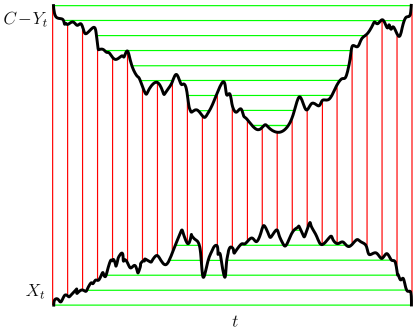

Constructing a sphere from a pair of trees

- X, Y ind. Brownian excursions on $[0, 1]$
- **Red**/**green** lines give an $\cong$-relation on $\mathbf{S}^2$
- Types of equivalence classes:
  1. Outer boundary of rectangle
  2. **V** line which does not share an endpoint with a **H** line
  3. **H** line below X or above $C - Y$ with two **V** lines with common endpoint
  4. **H** line below X or above $C - Y$ with two **V** lines with common endpoint and a third **V** line hitting in the middle
- $\cong$ is topologically closed and does not separate $\mathbf{S}^2$ into two or more components, thus $\mathbf{S}^2/\cong$ is homeomorphic to $\mathbf{S}^2$

H = horizontal, **V** = vertical

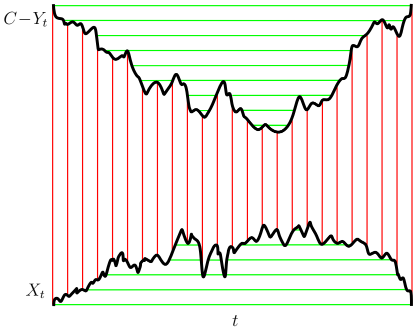

Constructing a sphere from a pair of trees

- X, Y ind. Brownian excursions on $[0,1]$
- **Red**/**green** lines give an $\cong$-relation on $\mathbf{S}^2$
- Types of equivalence classes:
  1. Outer boundary of rectangle
  2. **V** line which does not share an endpoint with a **H** line
  3. **H** line below X or above $C - Y$ with two **V** lines with common endpoint
  4. **H** line below X or above $C - Y$ with two **V** lines with common endpoint and a third **V** line hitting in the middle
- $\cong$ is topologically closed and does not separate $\mathbf{S}^2$ into two or more components, thus $\mathbf{S}^2/\cong$ is homeomorphic to $\mathbf{S}^2$
- Following the **V** lines from left to right gives a space-filling path on $\mathbf{S}^2/\cong$

H = horizontal, **V** = vertical

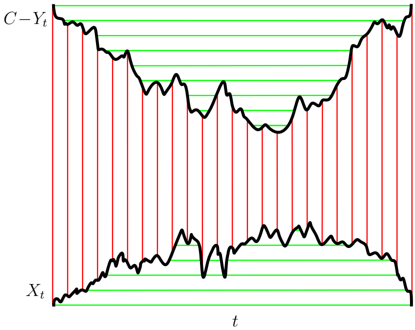

Constructing a sphere from a pair of trees

- X, Y ind. Brownian excursions on $[0, 1]$
- **Red**/**green** lines give an $\cong$-relation on $\mathbf{S}^2$
- Types of equivalence classes:
  1. Outer boundary of rectangle
  2. **V** line which does not share an endpoint with a **H** line
  3. **H** line below X or above $C - Y$ with two **V** lines with common endpoint
  4. **H** line below X or above $C - Y$ with two **V** lines with common endpoint and a third **V** line hitting in the middle
- $\cong$ is topologically closed and does not separate $\mathbf{S}^2$ into two or more components, thus $\mathbf{S}^2/\cong$ is homeomorphic to $\mathbf{S}^2$
- Following the **V** lines from left to right gives a space-filling path on $\mathbf{S}^2/\cong$

H = horizontal, **V** = vertical

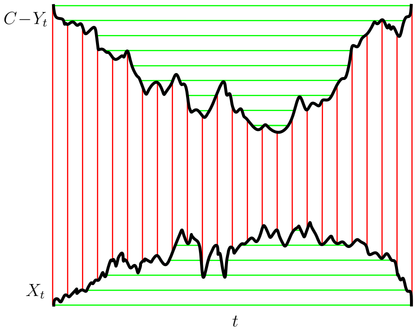

The sphere/space-filling path pair is a **peanoshere**

Constructing a sphere from a pair of trees

- X, Y ind. Brownian excursions on $[0,1]$
- **Red**/**green** lines give an $\cong$-relation on $\mathbf{S}^2$
- Types of equivalence classes:
  1. Outer boundary of rectangle
  2. **V** line which does not share an endpoint with a **H** line
  3. **H** line below X or above $C - Y$ with two **V** lines with common endpoint
  4. **H** line below X or above $C - Y$ with two **V** lines with common endpoint and a third **V** line hitting in the middle
- $\cong$ is topologically closed and does not separate $\mathbf{S}^2$ into two or more components, thus $\mathbf{S}^2/\cong$ is homeomorphic to $\mathbf{S}^2$
- Following the **V** lines from left to right gives a space-filling path on $\mathbf{S}^2/\cong$

H = horizontal, **V** = vertical

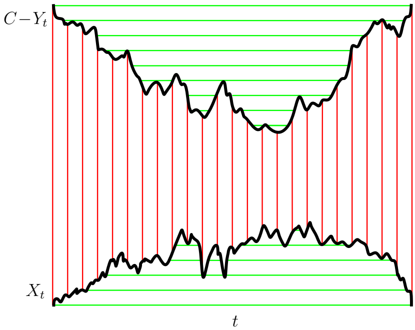

The sphere/space-filling path pair is a **peanoshere**

Q: What is the canonical embedding of this peanoshere into the Euclidean sphere $\mathbf{S}^2$?

Part II: Scaling limits of random planar maps and Liouville quantum gravity

Random planar maps

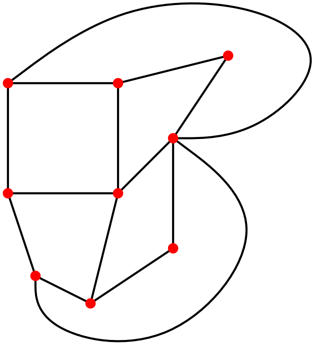

- A **planar map** is a finite graph together with an embedding in the plane so that no edges cross

Random planar maps

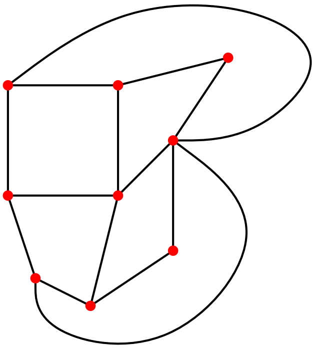

- A **planar map** is a finite graph together with an embedding in the plane so that no edges cross
- Its **faces** are the connected components of the complement of edges

Random planar maps

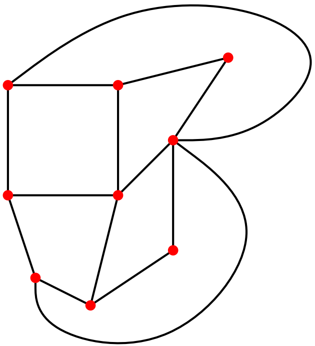

- A **planar map** is a finite graph together with an embedding in the plane so that no edges cross
- Its **faces** are the connected components of the complement of edges
- A map is a **quadrangulation** if each face has 4 adjacent edges

Random planar maps

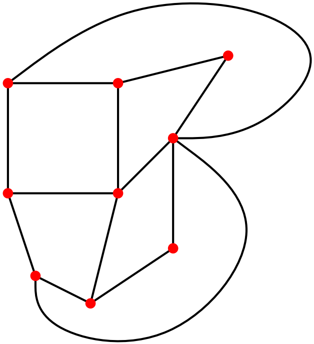

- A **planar map** is a finite graph together with an embedding in the plane so that no edges cross
- Its **faces** are the connected components of the complement of edges
- A map is a **quadrangulation** if each face has 4 adjacent edges
- Interested in **random quadrangulations** with n faces — **random planar map** (RPM).

Random planar maps

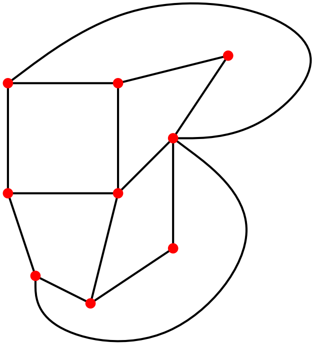

- A **planar map** is a finite graph together with an embedding in the plane so that no edges cross
- Its **faces** are the connected components of the complement of edges
- A map is a **quadrangulation** if each face has 4 adjacent edges
- Interested in **random quadrangulations** with n faces — **random planar map** (RPM).
- First studied by Tutte in 1960s while working on the four color theorem
  - **Combinatorics**: enumeration formulas
  - **Physics**: statistical physics models: percolation, Ising, UST ...
  - **Probability**: "uniformly random surface," Brownian surface

Random quadrangulation with 25,000 faces

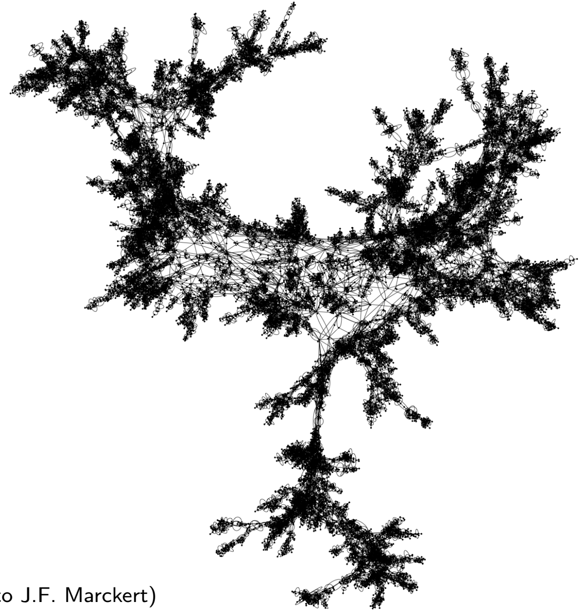

(Simulation due to J.F. Marckert)

Laws on quadrangulations

- Natural laws on quadrangulations with n faces.

Laws on quadrangulations

- Natural laws on quadrangulations with n faces.
  - Uniform measure

Laws on quadrangulations

- Natural laws on quadrangulations with n faces.
  - Uniform measure
  - Weighted by the partition function of the FK model with $q \in (0, 4)$:
    - For a fixed quadrangulation M, the probability of picking it is proportional to $\mathcal{Z}_M = \sum_L q^{\#L/2}$ where the sum is over loop configurations L and $\#L$ is the number of loops in L

Laws on quadrangulations

- Natural laws on quadrangulations with n faces.
  - Uniform measure
  - Weighted by the partition function of the FK model with $q \in (0,4)$:
    - For a fixed quadrangulation M, the probability of picking it is proportional to $\mathcal{Z}_M = \sum_L q^{\#L/2}$ where the sum is over loop configurations L and $\#L$ is the number of loops in L
- Natural to pick a map/loop-configuration pair (M, L) in the FK weighted case

Laws on quadrangulations

- Natural laws on quadrangulations with n faces.
  - Uniform measure
  - Weighted by the partition function of the FK model with $q \in (0, 4)$:
    - For a fixed quadrangulation M, the probability of picking it is proportional to $\mathcal{Z}_M = \sum_L q^{\#L/2}$ where the sum is over loop configurations L and $\#L$ is the number of loops in L
- Natural to pick a map/loop-configuration pair (M, L) in the FK weighted case
- Can encode the loops in terms of a tree/dual tree pair
  - Generate the tree by first picking a root
  - Generate the branch from the root to any vertex by following the boundaries of the loop configuration until the vertex is cut off from the root, at which point you branch towards the vertex and continue

Laws on quadrangulations

- Natural laws on quadrangulations with n faces.
  - Uniform measure
  - Weighted by the partition function of the FK model with $q \in (0,4)$:
    - For a fixed quadrangulation M, the probability of picking it is proportional to $\mathcal{Z}_M = \sum_L q^{\#L/2}$ where the sum is over loop configurations L and $\#L$ is the number of loops in L
- Natural to pick a map/loop-configuration pair (M, L) in the FK weighted case
- Can encode the loops in terms of a tree/dual tree pair
  - Generate the tree by first picking a root
  - Generate the branch from the root to any vertex by following the boundaries of the loop configuration until the vertex is cut off from the root, at which point you branch towards the vertex and continue

Sheffield's Hamburger-Cheeseburger (H-C) bijection encodes an FK-weighted planar map by describing the pair of contour functions which correspond to the tree/dual tree pair

Random quadrangulation

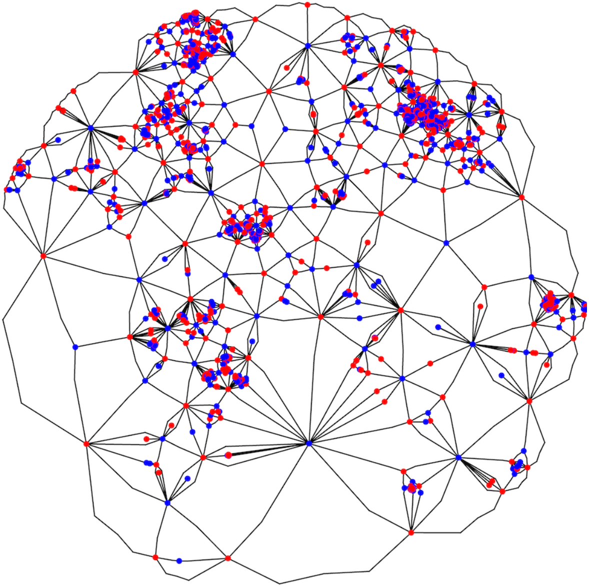

Sampled using H-C bijection.

Red tree

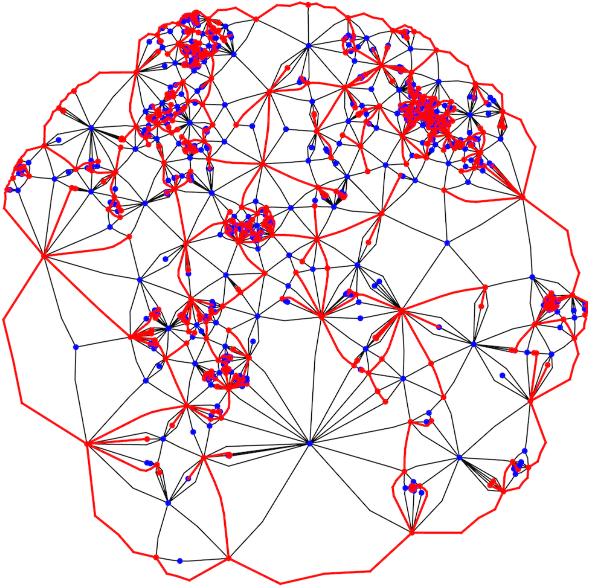

Sampled using H-C bijection.

Red and blue trees

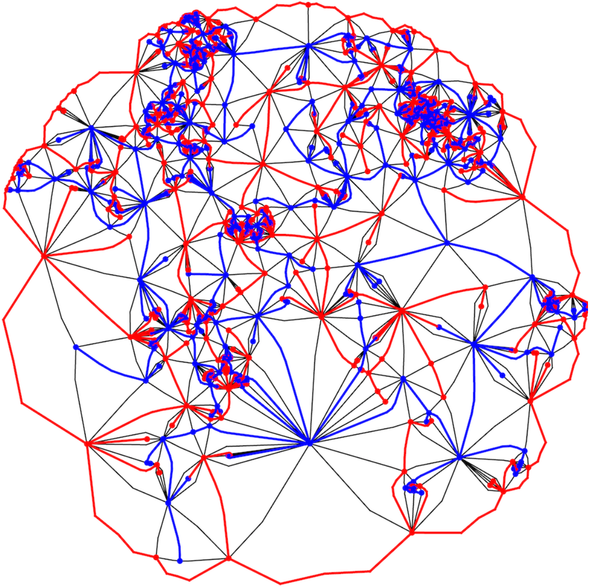

Sampled using H-C bijection.

Path snaking between the trees. Encodes the trees and how they are glued together.

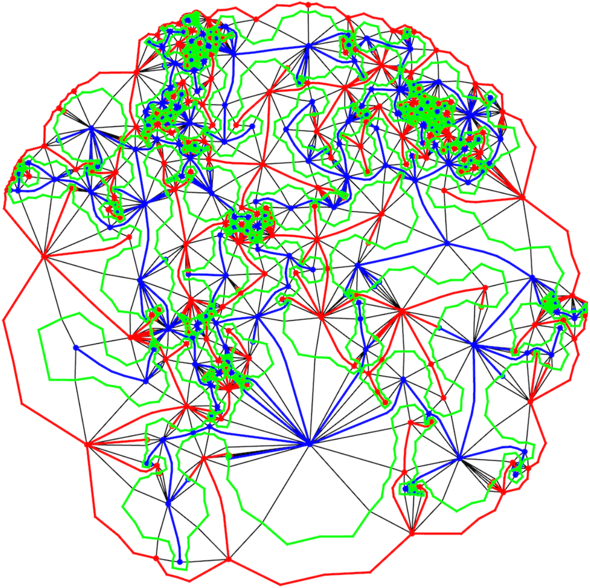

Sampled using H-C bijection.

How was the graph embedded into $\mathbf{R}^2$?

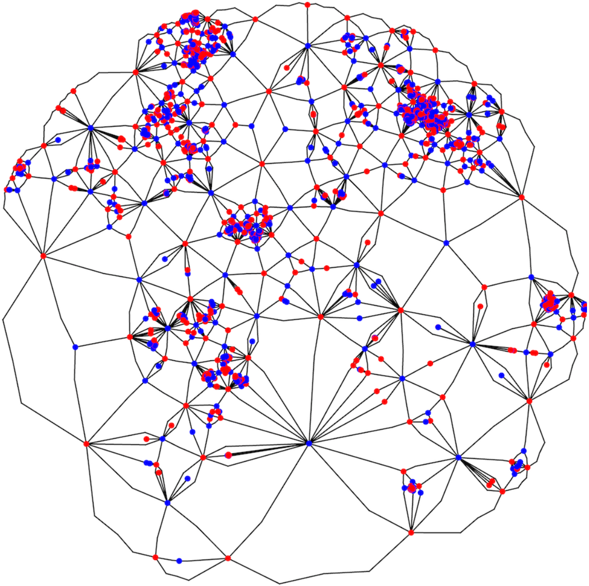

Sampled using H-C bijection.

Can subivide each quadrilateral to obtain a triangulation without multiple edges.

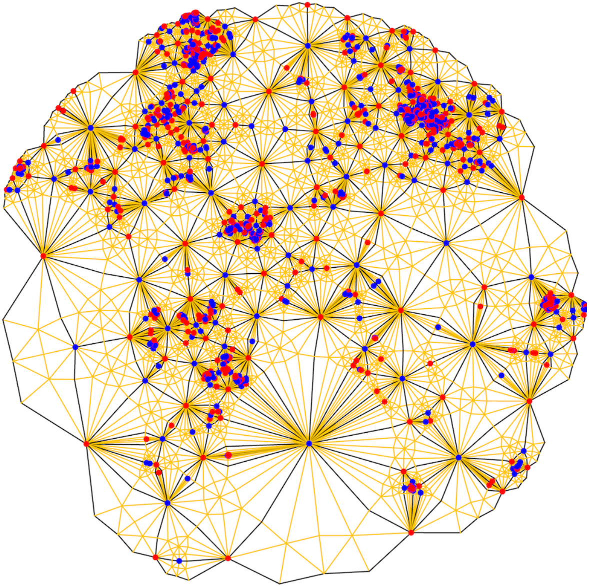

Sampled using H-C bijection.

Circle pack the resulting triangulation.

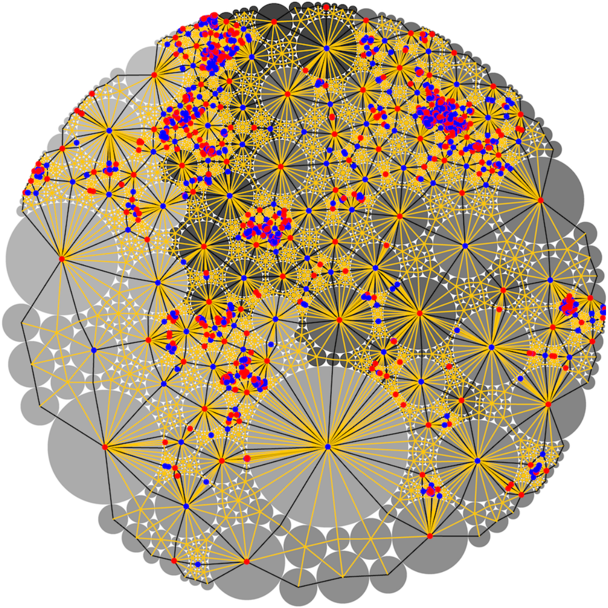

Sampled using H-C bijection. Packed with Stephenson's CirclePack.

Circle pack the resulting triangulation.

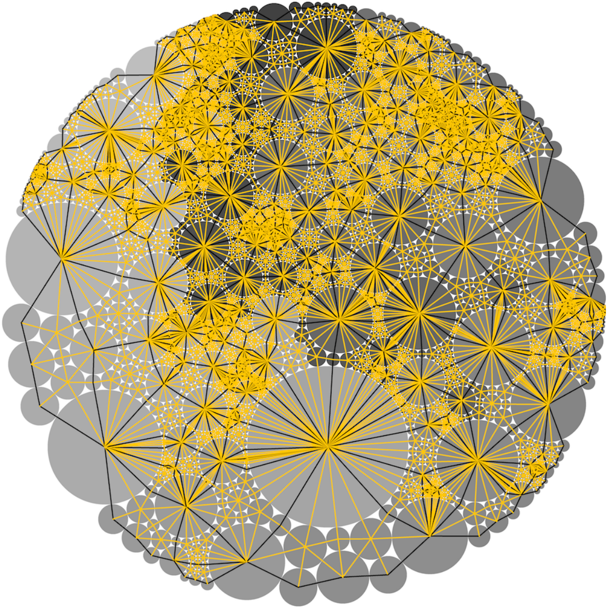

Sampled using H-C bijection. Packed with Stephenson's CirclePack.

Circle pack the resulting triangulation.

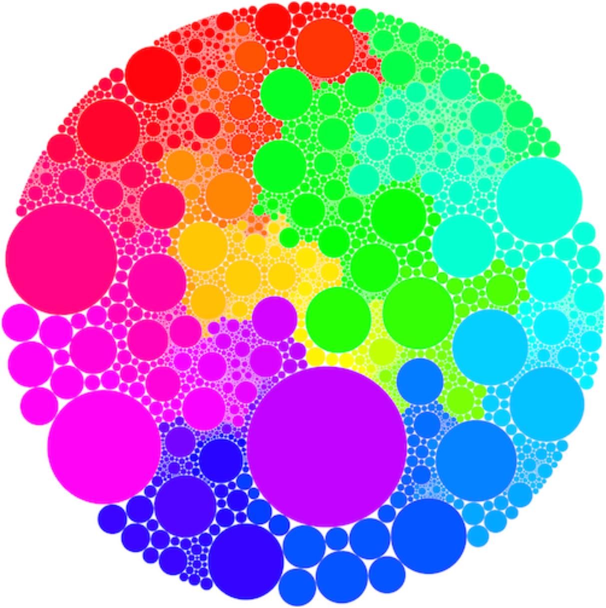

Sampled using H-C bijection. Packed with Stephenson's CirclePack.

What is the “limit” of this embedding? Circle packings are related to conformal maps.

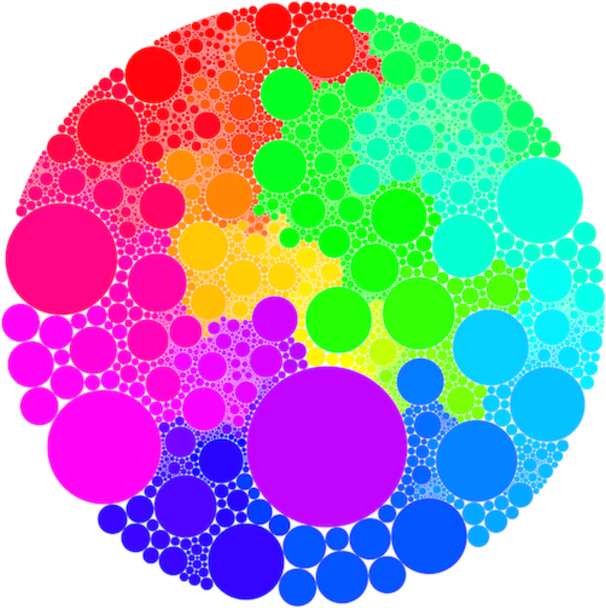

Sampled using H-C bijection. Packed with Stephenson’s CirclePack.

Random planar map convergence results

Uniformly random

- Diameter is $\asymp n^{1/4}$, profile of distances from random point (Chaissang-Schaefer)

Random planar map convergence results

Uniformly random

- Diameter is $\asymp n^{1/4}$, profile of distances from random point (Chaissang-Schaefer)
- Existence of subsequential limits after rescaling distances by $n^{-1/4}$ (Le Gall)

Random planar map convergence results

Uniformly random

- Diameter is $\asymp n^{1/4}$, profile of distances from random point (Chaissang-Schaefer)
- Existence of subsequential limits after rescaling distances by $n^{-1/4}$ (Le Gall)
- Existence of limit to the Brownian map (Le Gall, Miermont)

Random planar map convergence results

Uniformly random

- Diameter is $\asymp n^{1/4}$, profile of distances from random point (Chaissang-Schaefer)
- Existence of subsequential limits after rescaling distances by $n^{-1/4}$ (Le Gall)
- Existence of limit to the Brownian map (Le Gall, Miermont)

FK-weighted

Random planar map convergence results

Uniformly random

- Diameter is $\asymp n^{1/4}$, profile of distances from random point (Chaissang-Schaefer)
- Existence of subsequential limits after rescaling distances by $n^{-1/4}$ (Le Gall)
- Existence of limit to the Brownian map (Le Gall, Miermont)

FK-weighted

- H-C bijection encodes an FK weighted random planar map in terms of a pair of random discrete trees glued together along a space-filling path

Random planar map convergence results

Uniformly random

- Diameter is $\asymp n^{1/4}$, profile of distances from random point (Chaissang-Schaefer)
- Existence of subsequential limits after rescaling distances by $n^{-1/4}$ (Le Gall)
- Existence of limit to the Brownian map (Le Gall, Miermont)

FK-weighted

- H-C bijection encodes an FK weighted random planar map in terms of a pair of random discrete trees glued together along a space-filling path
- Sheffield proved that the contour functions of these two discrete trees properly rescaled converge to a pair of Brownian excursions

Random planar map convergence results

Uniformly random

- Diameter is $\asymp n^{1/4}$, profile of distances from random point (Chaissang-Schaefer)
- Existence of subsequential limits after rescaling distances by $n^{-1/4}$ (Le Gall)
- Existence of limit to the Brownian map (Le Gall, Miermont)

FK-weighted

- H-C bijection encodes an FK weighted random planar map in terms of a pair of random discrete trees glued together along a space-filling path
- Sheffield proved that the contour functions of these two discrete trees properly rescaled converge to a pair of Brownian excursions
- For UST weighted random planar maps ($q = 0$), the CRTs are independent. For general $q \in (0, 4)$, the CRTs are correlated

Random planar map convergence results

Uniformly random

- Diameter is $\asymp n^{1/4}$, profile of distances from random point (Chaissang-Schaefer)
- Existence of subsequential limits after rescaling distances by $n^{-1/4}$ (Le Gall)
- Existence of limit to the Brownian map (Le Gall, Miermont)

FK-weighted

- H-C bijection encodes an FK weighted random planar map in terms of a pair of random discrete trees glued together along a space-filling path
- Sheffield proved that the contour functions of these two discrete trees properly rescaled converge to a pair of Brownian excursions
- For UST weighted random planar maps ($q = 0$), the CRTs are independent. For general $q \in (0, 4)$, the CRTs are correlated
- Canonical embedding of peanospheres that come from gluing correlated CRTs is thus related to the problem of describing the scaling limits of FK weighted random planar maps embedded into $\mathbf{C} \cup \{\infty\}$

Liouville quantum gravity

- Liouville quantum gravity: $e^{\gamma h(z)} dz$ where h is a GFF and $\gamma \in [0,2)$

$\gamma = 0.5$

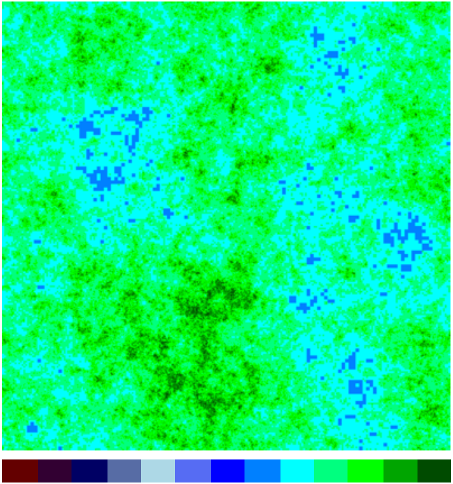

(Number of subdivisions)

Liouville quantum gravity

- Liouville quantum gravity: $e^{\gamma h(z)} dz$ where h is a GFF and $\gamma \in [0, 2)$
- Introduced by Polyakov in the 1980s as a generalization of the path integral to the setting of surfaces

$\gamma = 0.5$

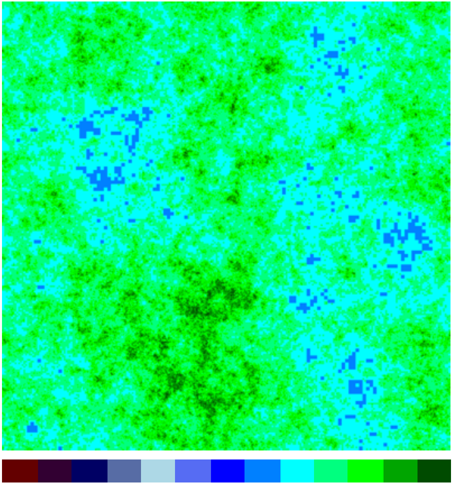

(Number of subdivisions)

Liouville quantum gravity

- Liouville quantum gravity: $e^{\gamma h(z)} dz$ where h is a GFF and $\gamma \in [0, 2)$
- Introduced by Polyakov in the 1980s as a generalization of the path integral to the setting of surfaces
- Does not make literal sense since h takes values in the space of distributions

$\gamma = 0.5$

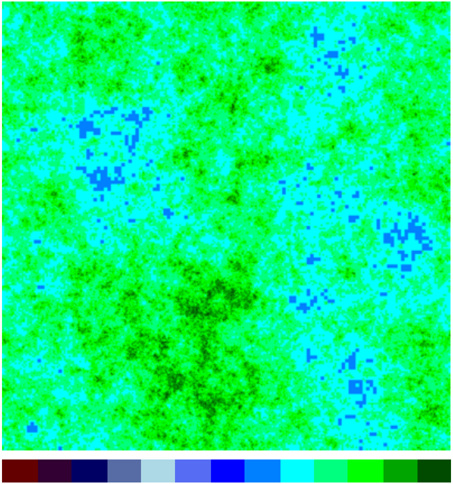

(Number of subdivisions)

Liouville quantum gravity

- Liouville quantum gravity: $e^{\gamma h(z)} dz$ where h is a GFF and $\gamma \in [0,2)$
- Introduced by Polyakov in the 1980s as a generalization of the path integral to the setting of surfaces
- Does not make literal sense since h takes values in the space of distributions
- Can be made sense of as a random area measure using a regularization procedure
    - Can compute areas of regions and lengths of curves

$\gamma = 0.5$

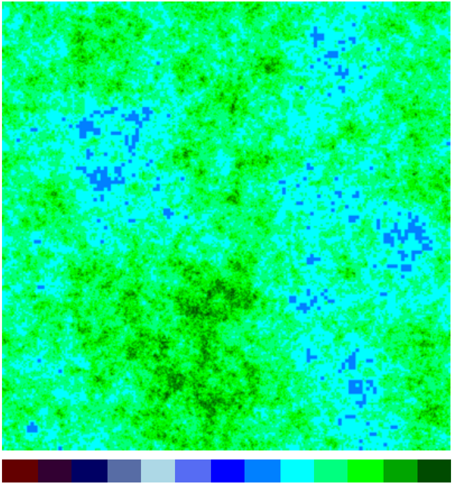

(Number of subdivisions)

Liouville quantum gravity

- Liouville quantum gravity: $e^{\gamma h(z)} dz$ where h is a GFF and $\gamma \in [0, 2)$
- Introduced by Polyakov in the 1980s as a generalization of the path integral to the setting of surfaces
- Does not make literal sense since h takes values in the space of distributions
- Can be made sense of as a random area measure using a regularization procedure
  - Can compute areas of regions and lengths of curves
- Conjectured to describe the limit of conformally embedded FK-weighted random planar maps

$\gamma = 0.5$

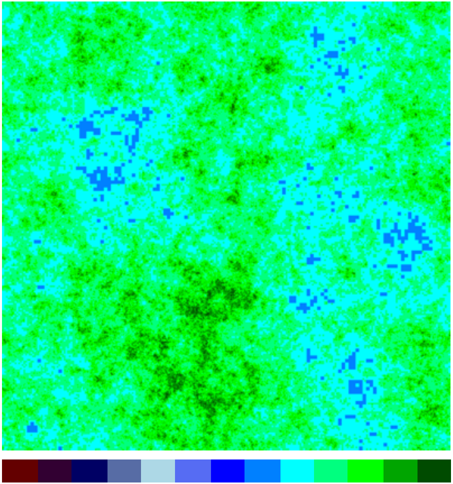

(Number of subdivisions)

Liouville quantum gravity

- Liouville quantum gravity: $e^{\gamma h(z)} dz$ where h is a GFF and $\gamma \in [0,2)$
- Introduced by Polyakov in the 1980s as a generalization of the path integral to the setting of surfaces
- Does not make literal sense since h takes values in the space of distributions
- Can be made sense of as a random area measure using a regularization procedure
  - Can compute areas of regions and lengths of curves
- Conjectured to describe the limit of conformally embedded FK-weighted random planar maps

$\gamma = 1.0$

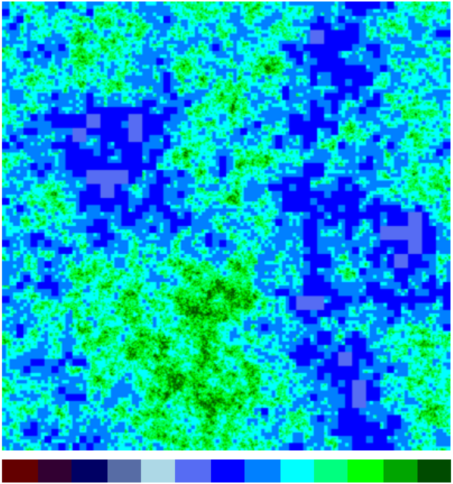

(Number of subdivisions)

Liouville quantum gravity

- Liouville quantum gravity: $e^{\gamma h(z)} dz$ where h is a GFF and $\gamma \in [0, 2)$
- Introduced by Polyakov in the 1980s as a generalization of the path integral to the setting of surfaces
- Does not make literal sense since h takes values in the space of distributions
- Can be made sense of as a random area measure using a regularization procedure
  - Can compute areas of regions and lengths of curves
- Conjectured to describe the limit of conformally embedded FK-weighted random planar maps

$\gamma = 1.5$

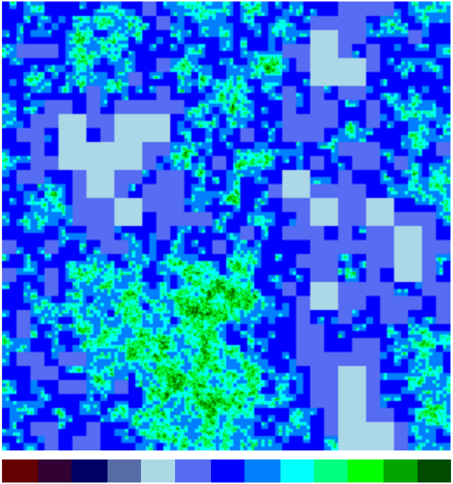

(Number of subdivisions)

Liouville quantum gravity

- Liouville quantum gravity: $e^{\gamma h(z)} dz$ where h is a GFF and $\gamma \in [0, 2)$
- Introduced by Polyakov in the 1980s as a generalization of the path integral to the setting of surfaces
- Does not make literal sense since h takes values in the space of distributions
- Can be made sense of as a random area measure using a regularization procedure
  - Can compute areas of regions and lengths of curves
- Conjectured to describe the limit of conformally embedded FK-weighted random planar maps

$\gamma = 2.0$

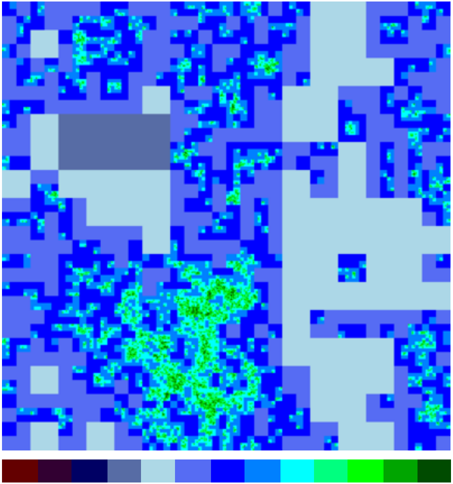

(Number of subdivisions)

Scaling limit conjectures

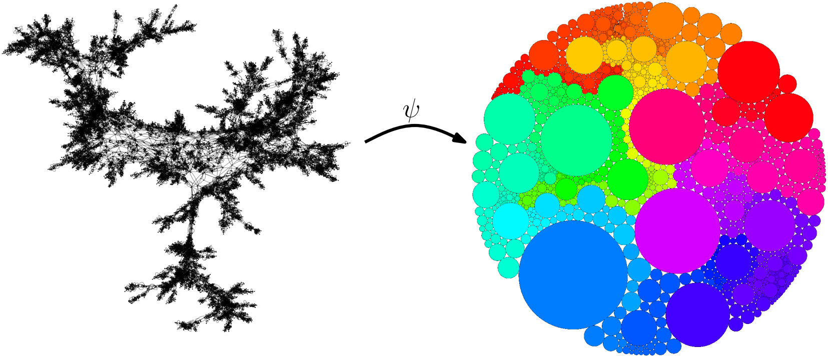

(Simulation due to J.-F. Marckert)

- Uniform RPM conformally embedded into $\mathbf{S}^2$ converges to $\sqrt{8/3}$-LQG as $n \to \infty$

Scaling limit conjectures

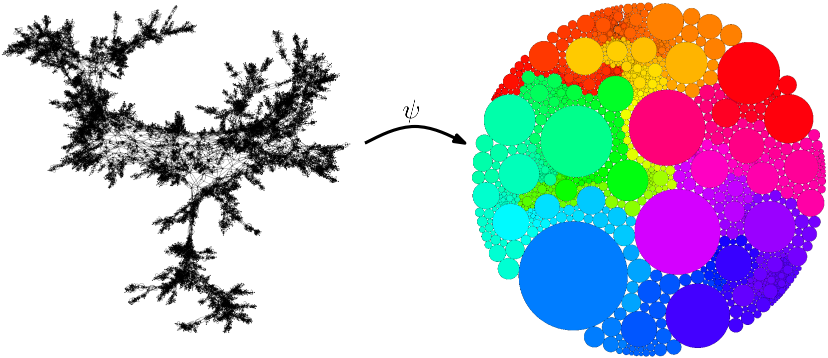

(Simulation due to J.-F. Marckert)

- Uniform RPM conformally embedded into $\mathbf{S}^2$ converges to $\sqrt{8/3}$-LQG as $n \to \infty$
- For $q \in [0,4)$, FK weighted RPM together with loop configuration conformally embedded into $\mathbf{S}^2$ converges to γ-LQG as $n \to \infty$ decorated by an independent $\mathrm{CLE}_{\kappa'}$ where

$$q = 2 + 2\cos\frac{8\pi}{\kappa'}, \quad \gamma = \sqrt{16/\kappa'} \in [\sqrt{2}, 2), \quad \kappa' \in (4,8].$$

Part III: Results

Main result

Theorem (Duplantier, M., Sheffield)

For each $\gamma \in (0,2)$ there is a type of γ-LQG surface such that the following are true:

Main result

Theorem (Duplantier, M., Sheffield)

For each $\gamma \in (0,2)$ there is a type of γ-LQG surface such that the following are true:

- *If we explore with an independent space-filling $\mathrm{SLE}_{\kappa'}$ process, $\kappa' = \frac{16}{\gamma^2}$, then the LQG lengths of its left and right sides evolve as a $2D$ Brownian motion (L, R)*

Main result

Theorem (Duplantier, M., Sheffield)

For each $\gamma \in (0,2)$ *there is a type of* γ*-LQG surface such that the following are true:*

- *If we explore with an independent space-filling* $\mathrm{SLE}_{\kappa'}$ *process,* $\kappa' = \frac{16}{\gamma^2}$*, then the LQG lengths of its left and right sides evolve as a* $2D$ *Brownian motion* (L, R)
- (L, R) *almost surely determine both the* γ*-LQG surface and the* $\mathrm{SLE}_{\kappa'}$

Main result

Theorem (Duplantier, M., Sheffield)

For each $\gamma \in (0,2)$ there is a type of γ-LQG surface such that the following are true:

- *If we explore with an independent space-filling $\mathrm{SLE}_{\kappa'}$ process, $\kappa' = \frac{16}{\gamma^2}$, then the LQG lengths of its left and right sides evolve as a 2D Brownian motion (L,R)*
- *(L,R) almost surely determine both the γ-LQG surface and the $\mathrm{SLE}_{\kappa'}$*

Comments

Main result

Theorem (Duplantier, M., Sheffield)

For each $\gamma \in (0,2)$ there is a type of γ-LQG surface such that the following are true:

- *If we explore with an independent space-filling $\mathrm{SLE}_{\kappa'}$ process, $\kappa' = \frac{16}{\gamma^2}$, then the LQG lengths of its left and right sides evolve as a 2D Brownian motion (L, R)*
- *(L, R) almost surely determine both the γ-LQG surface and the $\mathrm{SLE}_{\kappa'}$*

Comments

- Space-filling $\mathrm{SLE}_{\kappa'}$ is the peano curve associated with the continuum tree/dual tree pair which encodes $\mathrm{CLE}_{\kappa'}$

Main result

Theorem (Duplantier, M., Sheffield)

For each $\gamma \in (0,2)$ there is a type of γ-LQG surface such that the following are true:

- *If we explore with an independent space-filling $\mathrm{SLE}_{\kappa'}$ process, $\kappa' = \frac{16}{\gamma^2}$, then the LQG lengths of its left and right sides evolve as a 2D Brownian motion (L, R)*
- *(L, R) almost surely determine both the γ-LQG surface and the $\mathrm{SLE}_{\kappa'}$*

Comments

- Space-filling $\mathrm{SLE}_{\kappa'}$ is the peano curve associated with the continuum tree/dual tree pair which encodes $\mathrm{CLE}_{\kappa'}$
- Combined with the convergence for the H-C bijection, this says that FK weighted RPM converge to CLE-decorated LQG with respect to the topology where two loop-decorated surfaces are close if the contour functions of their tree/dual tree pair are close

Main result

Theorem (Duplantier, M., Sheffield)

For each $\gamma \in (0,2)$ there is a type of γ-LQG surface such that the following are true:

- *If we explore with an independent space-filling $\mathrm{SLE}_{\kappa'}$ process, $\kappa' = \frac{16}{\gamma^2}$, then the LQG lengths of its left and right sides evolve as a 2D Brownian motion (L, R)*
- *(L, R) almost surely determine both the γ-LQG surface and the $\mathrm{SLE}_{\kappa'}$*

Comments

- Space-filling $\mathrm{SLE}_{\kappa'}$ is the peano curve associated with the continuum tree/dual tree pair which encodes $\mathrm{CLE}_{\kappa'}$
- Combined with the convergence for the H-C bijection, this says that FK weighted RPM converge to CLE-decorated LQG with respect to the topology where two loop-decorated surfaces are close if the contour functions of their tree/dual tree pair are close
- For planar lattices, the FK models which have been shown to converge to SLE are the UST ($q = 0$), percolation ($q = 1$), FK-Ising model ($q = 2$) (Lawler-Schramm-Werner, Smirnov).

Main result

Theorem (Duplantier, M., Sheffield)

For each $\gamma \in (0,2)$ there is a type of γ-LQG surface such that the following are true:

- *If we explore with an independent space-filling $\mathrm{SLE}_{\kappa'}$ process, $\kappa' = \frac{16}{\gamma^2}$, then the LQG lengths of its left and right sides evolve as a 2D Brownian motion (L, R)*
- *(L, R) almost surely determine both the γ-LQG surface and the $\mathrm{SLE}_{\kappa'}$*

Comments

- Space-filling $\mathrm{SLE}_{\kappa'}$ is the peano curve associated with the continuum tree/dual tree pair which encodes $\mathrm{CLE}_{\kappa'}$
- Combined with the convergence for the H-C bijection, this says that FK weighted RPM converge to CLE-decorated LQG with respect to the topology where two loop-decorated surfaces are close if the contour functions of their tree/dual tree pair are close
- For planar lattices, the FK models which have been shown to converge to SLE are the UST $(q = 0)$, percolation $(q = 1)$, FK-Ising model $(q = 2)$ (Lawler-Schramm-Werner, Smirnov).
- The above result implies the convergence *for all $q \in [0,4)$* on RPM to $\mathrm{SLE}_{\kappa'}$ with

$$q = 2 + 2\cos\frac{8\pi}{\kappa'}, \quad \gamma = \sqrt{16/\kappa'} \in [\sqrt{2}, 2), \quad \kappa' \in (4, 8].$$

Main result

Theorem (Duplantier, M., Sheffield)

For each $\gamma \in (0,2)$ there is a type of γ-LQG surface such that the following are true:

- *If we explore with an independent space-filling $\mathrm{SLE}_{\kappa'}$ process, $\kappa' = \frac{16}{\gamma^2}$, then the LQG lengths of its left and right sides evolve as a 2D Brownian motion (L, R)*
- *(L, R) almost surely determine both the γ-LQG surface and the $\mathrm{SLE}_{\kappa'}$*

Comments

- Space-filling $\mathrm{SLE}_{\kappa'}$ is the peano curve associated with the continuum tree/dual tree pair which encodes $\mathrm{CLE}_{\kappa'}$
- Combined with the convergence for the H-C bijection, this says that FK weighted RPM converge to CLE-decorated LQG with respect to the topology where two loop-decorated surfaces are close if the contour functions of their tree/dual tree pair are close
- For planar lattices, the FK models which have been shown to converge to SLE are the UST $(q = 0)$, percolation $(q = 1)$, FK-Ising model $(q = 2)$ (Lawler-Schramm-Werner, Smirnov).
- The above result implies the convergence *for all $q \in [0,4)$* on RPM to $\mathrm{SLE}_{\kappa'}$ with

$$q = 2 + 2\cos\frac{8\pi}{\kappa'}, \quad \gamma = \sqrt{16/\kappa'} \in [\sqrt{2}, 2), \quad \kappa' \in (4, 8].$$

- As in the discrete setting, the contour functions of the continuum tree/dual tree pair determine everything

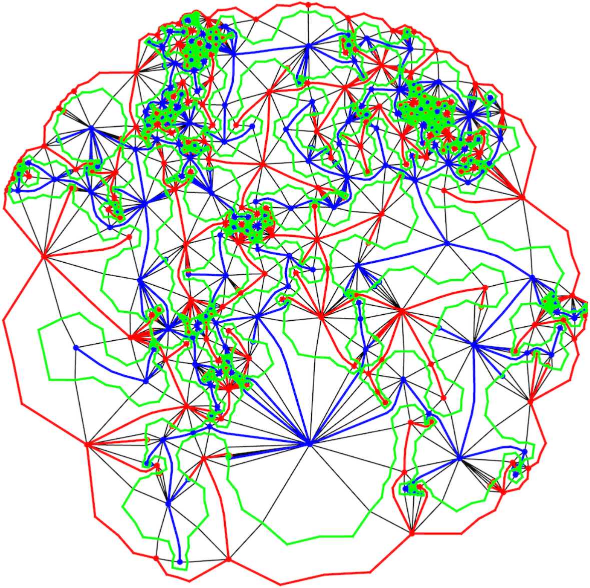

Random quadrangulation as a gluing of trees

Continuum space-filling path

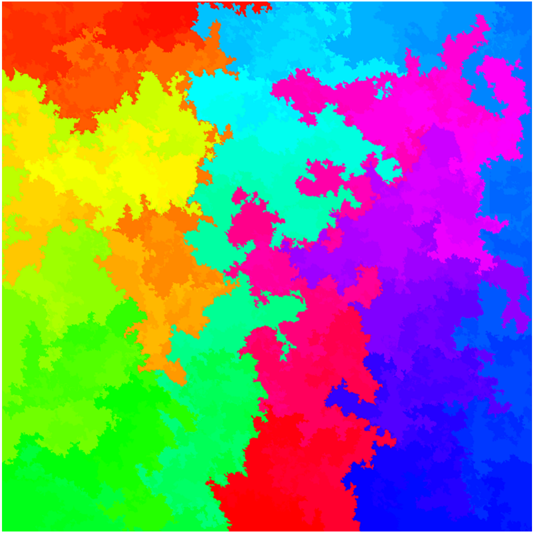

Space-filling SLE_6 on a LQG surface. Random path which encodes the limit of a RPM.

A calculus of random surfaces

- **Types of surfaces:** quantum wedges, cones, disks, and spheres
- **Operations:** welding and cutting
- Interfaces between welded surfaces are variants of SLE which can be described as GFF flow lines
- Conversely, natural to cut these surfaces with SLE-type paths

External inputs

Imaginary geometry: calculus of flow lines of $e^{ih/\chi}$ where h is a GFF.

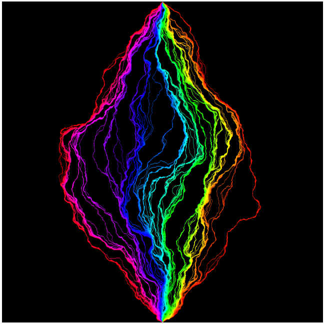

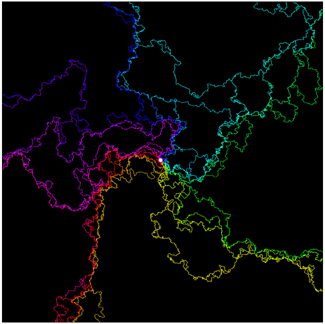

Paths are types of SLE curves. Regions between paths are independent wedges.

External inputs

Imaginary geometry: calculus of flow lines of $e^{ih/\chi}$ where h is a GFF.

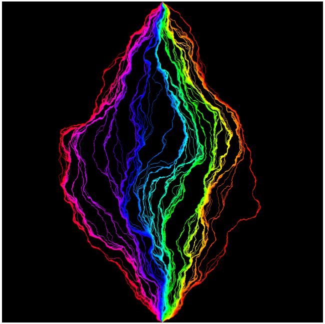

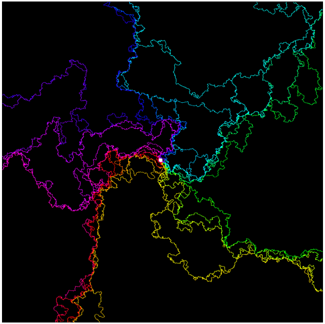

Paths are types of SLE curves. Regions between paths are independent wedges.

Conformal welding: Certain special case of "quantum wedge welding" due to Sheffield. Interface almost surely determined by welding, lengths on left and right sides of interface almost surely agree.

Types of random surfaces

Quantum wedges

- Start with a free boundary GFF h on a Euclidean wedge $\mathbf{W}_\theta$ with angle θ

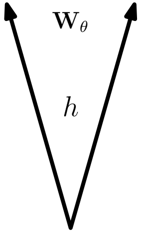

Types of random surfaces

Quantum wedges

- Start with a free boundary GFF h on a Euclidean wedge $\mathbf{W}_\theta$ with angle θ
- Change coordinates to $\mathbf{H}$ with $z^{\theta/\pi}$. Yields free boundary GFF plus $Q(\frac{\theta}{\pi} - 1) \log |z|$

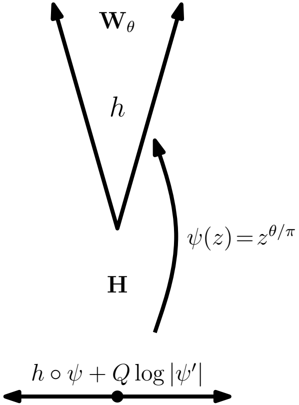

Types of random surfaces

Quantum wedges

- Start with a free boundary GFF h on a Euclidean wedge $\mathbf{W}_\theta$ with angle θ
- Change coordinates to $\mathbf{H}$ with $z^{\theta/\pi}$. Yields free boundary GFF plus $Q(\frac{\theta}{\pi}-1)\log|z|$
- Defined modulo global additive constant; fix additive constant in canonical way

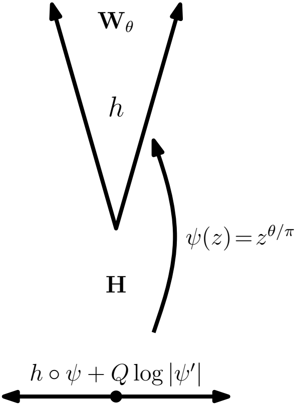

Types of random surfaces

Quantum wedges

- Start with a free boundary GFF h on a Euclidean wedge $\mathbf{W}_\theta$ with angle θ
- Change coordinates to $\mathbf{H}$ with $z^{\theta/\pi}$. Yields free boundary GFF plus $Q(\frac{\theta}{\pi}-1)\log|z|$
- Defined modulo global additive constant; fix additive constant in canonical way
- Parameterize space of wedges by multiple α of $-\log|z|$ or by weight $W = \gamma(\gamma + \frac{2}{\gamma} - \alpha)$

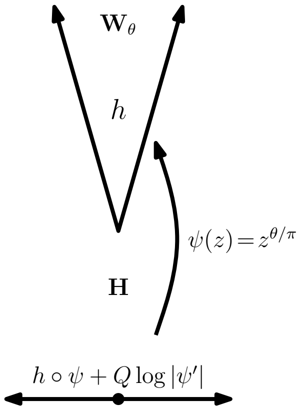

Types of random surfaces

Quantum wedges

- Start with a free boundary GFF h on a Euclidean wedge $\mathbf{W}_\theta$ with angle θ
- Change coordinates to $\mathbf{H}$ with $z^{\theta/\pi}$. Yields free boundary GFF plus $Q(\frac{\theta}{\pi}-1)\log|z|$
- Defined modulo global additive constant; fix additive constant in canonical way
- Parameterize space of wedges by multiple α of $-\log|z|$ or by weight $W=\gamma(\gamma+\frac{2}{\gamma}-\alpha)$

Quantum cones

- Similar to a wedge except start with a GFF on a Euclidean cone with angle θ
- Parameterize space of cones with multiple α of $-\log|z|$ or by weight $W=2\gamma(Q-\alpha)$

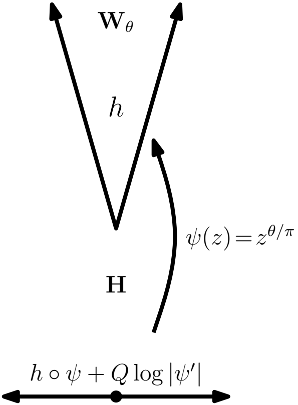

Types of random surfaces

Quantum wedges

- Start with a free boundary GFF h on a Euclidean wedge $\mathbf{W}_\theta$ with angle θ
- Change coordinates to $\mathbf{H}$ with $z^{\theta/\pi}$. Yields free boundary GFF plus $Q(\frac{\theta}{\pi}-1)\log|z|$
- Defined modulo global additive constant; fix additive constant in canonical way
- Parameterize space of wedges by multiple α of $-\log|z|$ or by weight $W = \gamma(\gamma + \frac{2}{\gamma} - \alpha)$

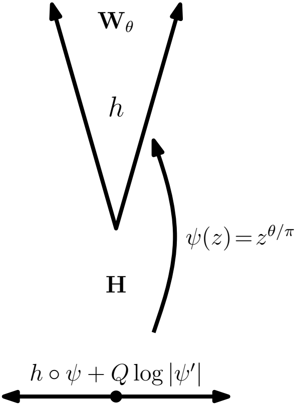

Quantum cones

- Similar to a wedge except start with a GFF on a Euclidean cone with angle θ
- Parameterize space of cones with multiple α of $-\log|z|$ or by weight $W = 2\gamma(Q - \alpha)$

Quantum disks and spheres (finite volume surfaces)

- Constructed with free boundary GFF and Bessel excursion measures

Welding and slicing independent wedges

Can "weld" and "slice" quantum wedges to obtain larger/smaller wedges.

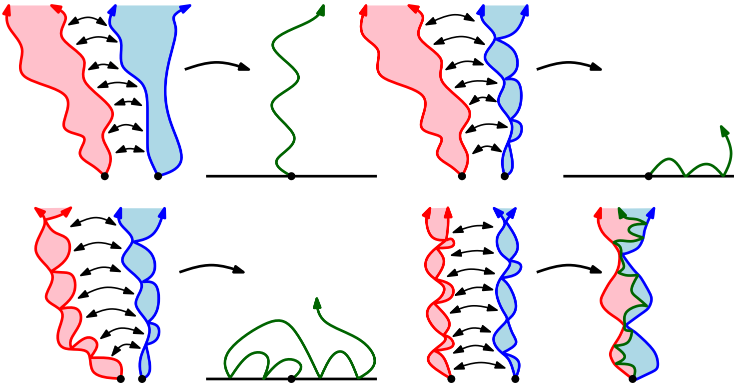

- Weight parameter $W = \gamma(\gamma + \frac{2}{\gamma} - \alpha)$ is additive under the welding operation.
- Interface between welding of independent wedges $\mathcal{W}_1, \mathcal{W}_2$ of weight W_1 and W_2 is an $\mathrm{SLE}_\kappa(W_1 - 2; W_2 - 2)$.
- Interface is a deterministic function of $\mathcal{W}_1, \mathcal{W}_2$.

Welding many wedges

Can also weld together many wedges $\mathcal{W}_1, \ldots, \mathcal{W}_n$ of weight $W_1, \ldots, W_n$ to obtain a wedge $\mathcal{W}$ with weight $W_1 + \cdots + W_n$.

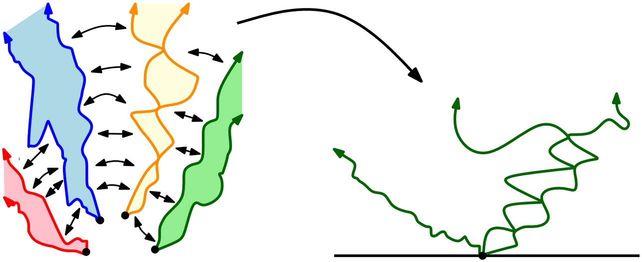

Interfaces are $\mathrm{SLE}_\kappa(\rho_1; \rho_2)$ type processes coupled together as flow lines of a GFF and are a deterministic function of $\mathcal{W}_1, \ldots, \mathcal{W}_n$.

Welding a wedge to itself

Can "weld" left and right sides of a wedge to obtain a cone. Conversely, can slice a cone with an independent SLE to obtain a wedge.

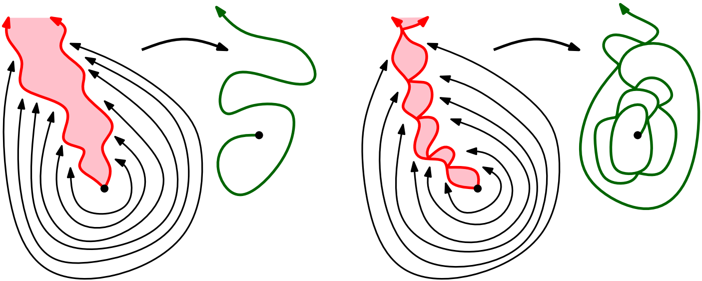

- Weight parameter $W = 2\gamma(Q - \alpha)$
- Welding left and right sides of weight W wedge yields a weight W cone; the interface is an independent whole-plane $\mathrm{SLE}_\kappa(W-2)$
- Interface is simple if the wedge is "thick" as on the left (homeomorphic to **H**); it is self-intersecting if the wedge is thin as on the right (not homeomorphic to **H**)

Exploring an LQG surface with an $\mathrm{SLE}_{\kappa'}$ with $\kappa' \in (4, 8)$

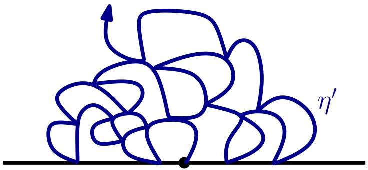

- Draw an independent $\mathrm{SLE}_{\kappa'}$ on top of a $\frac{3\gamma^2}{2} - 2$ wedge, $\gamma = 4/\sqrt{\kappa'}$

Exploring an LQG surface with an $\mathrm{SLE}_{\kappa'}$ with $\kappa' \in (4,8)$

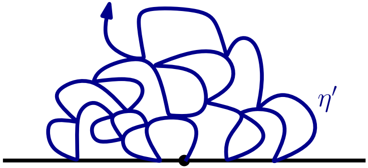

- Draw an independent $\mathrm{SLE}_{\kappa'}$ on top of a $\frac{3\gamma^2}{2} - 2$ wedge, $\gamma = 4/\sqrt{\kappa'}$
- Quantum disks cut out by the path have a Poissonian structure

Exploring an LQG surface with an $\mathrm{SLE}_{\kappa'}$ with $\kappa' \in (4,8)$

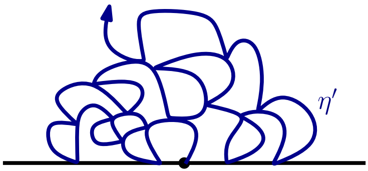

- Draw an independent $\mathrm{SLE}_{\kappa'}$ on top of a $\frac{3\gamma^2}{2} - 2$ wedge, $\gamma = 4/\sqrt{\kappa'}$
- Quantum disks cut out by the path have a Poissonian structure
- Conditionally independent given their boundary lengths

Exploring an LQG surface with an $\mathrm{SLE}_{\kappa'}$ with $\kappa' \in (4,8)$

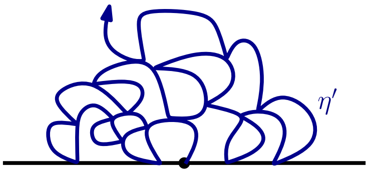

- Draw an independent $\mathrm{SLE}_{\kappa'}$ on top of a $\frac{3\gamma^2}{2} - 2$ wedge, $\gamma = 4/\sqrt{\kappa'}$
- Quantum disks cut out by the path have a Poissonian structure
- Conditionally independent given their boundary lengths
- Change in the left/right γ-LQG boundary lengths given by independent $\frac{\kappa'}{4}$-stable Lévy processes

Exploring an LQG surface with an $\mathrm{SLE}_{\kappa'}$ with $\kappa' \in (4, 8)$

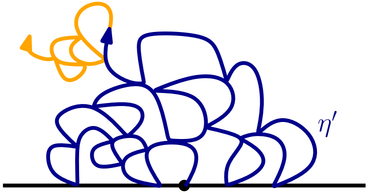

- Draw an independent $\mathrm{SLE}_{\kappa'}$ on top of a $\frac{3\gamma^2}{2} - 2$ wedge, $\gamma = 4/\sqrt{\kappa'}$
- Quantum disks cut out by the path have a Poissonian structure
- Conditionally independent given their boundary lengths
- Change in the left/right γ-LQG boundary lengths given by independent $\frac{\kappa'}{4}$-stable Lévy processes

Exploring an LQG surface with an $\mathrm{SLE}_{\kappa'}$ with $\kappa' \in (4, 8)$

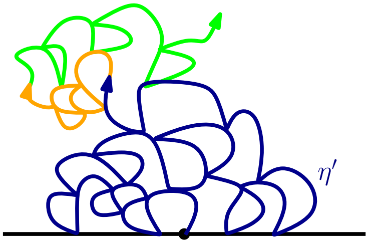

- Draw an independent $\mathrm{SLE}_{\kappa'}$ on top of a $\frac{3\gamma^2}{2} - 2$ wedge, $\gamma = 4/\sqrt{\kappa'}$
- Quantum disks cut out by the path have a Poissonian structure
- Conditionally independent given their boundary lengths
- Change in the left/right γ-LQG boundary lengths given by independent $\frac{\kappa'}{4}$-stable Lévy processes

Exploring an LQG surface with an $\mathrm{SLE}_{\kappa'}$ with $\kappa' \in (4, 8)$

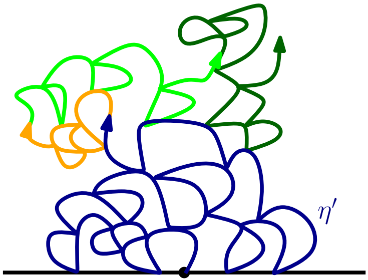

- Draw an independent $\mathrm{SLE}_{\kappa'}$ on top of a $\frac{3\gamma^2}{2} - 2$ wedge, $\gamma = 4/\sqrt{\kappa'}$
- Quantum disks cut out by the path have a Poissonian structure
- Conditionally independent given their boundary lengths
- Change in the left/right γ-LQG boundary lengths given by independent $\frac{\kappa'}{4}$-stable Lévy processes

Exploring an LQG surface with an $\mathrm{SLE}_{\kappa'}$ with $\kappa' \in (4,8)$

- Draw an independent $\mathrm{SLE}_{\kappa'}$ on top of a $\frac{3\gamma^2}{2} - 2$ wedge, $\gamma = 4/\sqrt{\kappa'}$
- Quantum disks cut out by the path have a Poissonian structure
- Conditionally independent given their boundary lengths
- Change in the left/right γ-LQG boundary lengths given by independent $\frac{\kappa'}{4}$-stable Lévy processes

Gluing independent Lévy trees

Can view $\mathrm{SLE}_{\kappa'}$ process, $\kappa' \in (4,8)$ as a gluing of two $\frac{\kappa'}{4}$-stable Lévy trees.

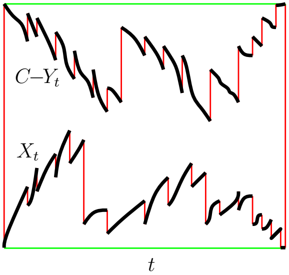

Gluing independent Lévy trees

Can view $\mathrm{SLE}_{\kappa'}$ process, $\kappa' \in (4,8)$ as a gluing of two $\frac{\kappa'}{4}$-stable Lévy trees.

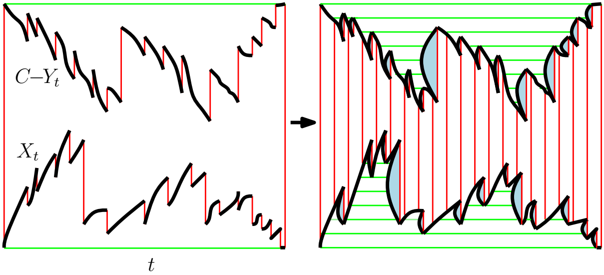

Gluing independent Lévy trees

Can view $\mathrm{SLE}_{\kappa'}$ process, $\kappa' \in (4,8)$ as a gluing of two $\frac{\kappa'}{4}$-stable Lévy trees.

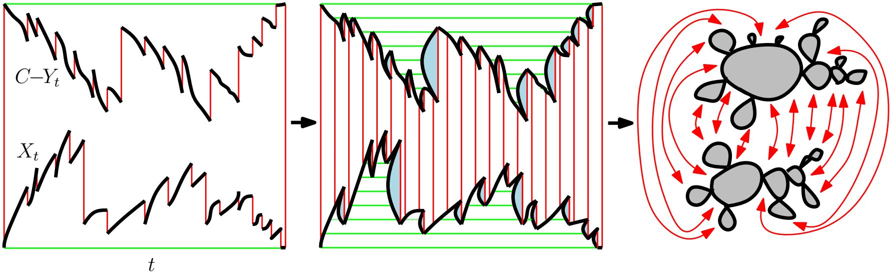

Gluing independent Lévy trees

Can view $\mathrm{SLE}_{\kappa'}$ process, $\kappa' \in (4,8)$ as a gluing of two $\frac{\kappa'}{4}$-stable Lévy trees.

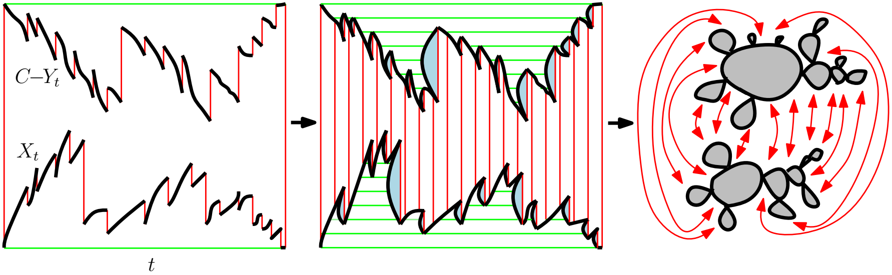

- The two trees of quantum disks almost surely determine both the $\mathrm{SLE}_{\kappa'}$ and the LQG surface on which it is drawn

Gluing independent Lévy trees

Can view $\mathrm{SLE}_{\kappa'}$ process, $\kappa' \in (4,8)$ as a gluing of two $\frac{\kappa'}{4}$-stable Lévy trees.

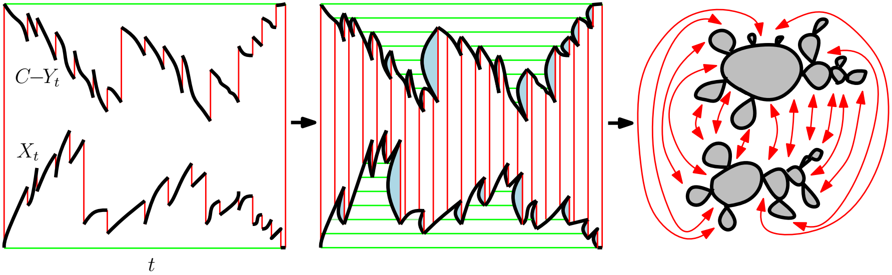

- The two trees of quantum disks almost surely determine both the $\mathrm{SLE}_{\kappa'}$ and the LQG surface on which it is drawn
- Can convert questions about $\mathrm{SLE}_{\kappa'}$ into questions about $\frac{\kappa'}{4}$-stable processes

Gluing independent Lévy trees

Can view $\mathrm{SLE}_{\kappa'}$ process, $\kappa' \in (4,8)$ as a gluing of two $\frac{\kappa'}{4}$-stable Lévy trees.

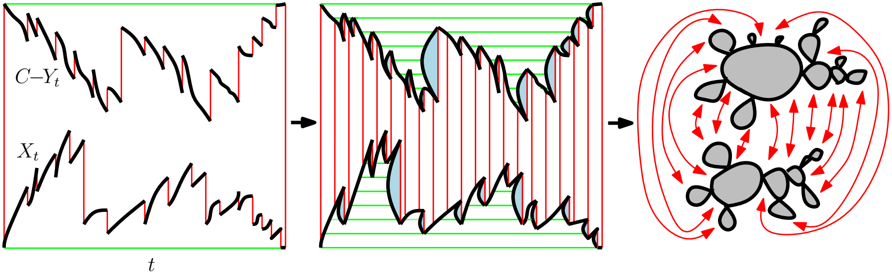

- The two trees of quantum disks almost surely determine both the $\mathrm{SLE}_{\kappa'}$ and the LQG surface on which it is drawn
- Can convert questions about $\mathrm{SLE}_{\kappa'}$ into questions about $\frac{\kappa'}{4}$-stable processes
- **Question:** Is the graph of components of an $\mathrm{SLE}_{\kappa'}$ process connected?

Gluing independent Lévy trees

Can view $\mathrm{SLE}_{\kappa'}$ process, $\kappa' \in (4,8)$ as a gluing of two $\frac{\kappa'}{4}$-stable Lévy trees.

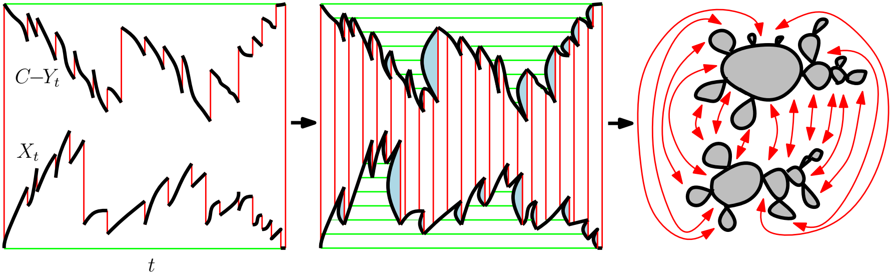

- The two trees of quantum disks almost surely determine both the $\mathrm{SLE}_{\kappa'}$ and the LQG surface on which it is drawn
- Can convert questions about $\mathrm{SLE}_{\kappa'}$ into questions about $\frac{\kappa'}{4}$-stable processes
- **Question:** Is the graph of components of an $\mathrm{SLE}_{\kappa'}$ process connected?
- **Equivalently:** If we glue together two independent $\frac{\kappa'}{4}$-stable trees as above, is it possible to get from one jump to any other by passing through a finite number of $\cong$-classes?

Discrete intuition

Welding/cutting results may seem to be a bizarre coincidence at first sight. However, results of this type are very natural in view of conjectures connecting LQG and random planar maps.

"Domain Markov half planar" map with marked boundary edge. Vertices to the left and right of edge colored red and blue.

Discrete intuition

Welding/cutting results may seem to be a bizarre coincidence at first sight. However, results of this type are very natural in view of conjectures connecting LQG and random planar maps.

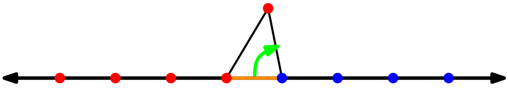

“Domain Markov half planar” map with marked boundary edge. Vertices to the left and right of edge colored red and blue. Percolation exploration from marked edge

Discrete intuition

Welding/cutting results may seem to be a bizarre coincidence at first sight. However, results of this type are very natural in view of conjectures connecting LQG and random planar maps.

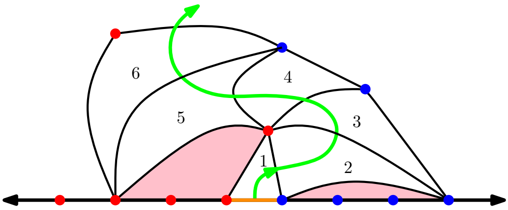

"Domain Markov half planar" map with marked boundary edge. Vertices to the left and right of edge colored red and blue. Percolation exploration from marked edge

Discrete intuition

Welding/cutting results may seem to be a bizarre coincidence at first sight. However, results of this type are very natural in view of conjectures connecting LQG and random planar maps.

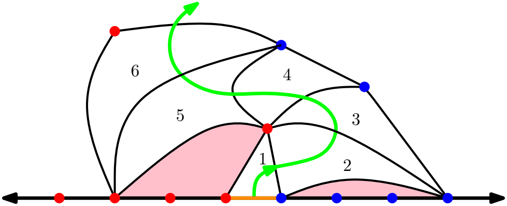

"Domain Markov half planar" map with marked boundary edge. Vertices to the left and right of edge colored red and blue. Percolation exploration from marked edge

- Left and right boundary lengths evolve independently and have independent increments

Discrete intuition

Welding/cutting results may seem to be a bizarre coincidence at first sight. However, results of this type are very natural in view of conjectures connecting LQG and random planar maps.

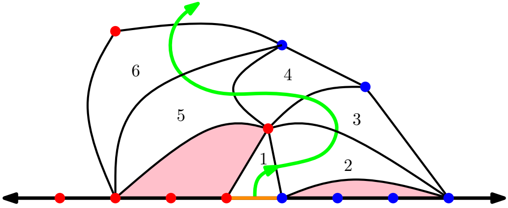

"Domain Markov half planar" map with marked boundary edge. Vertices to the left and right of edge colored red and blue. Percolation exploration from marked edge

- Left and right boundary lengths evolve independently and have independent increments
- Components cut off from infinity have i.i.d. structure

Discrete intuition

Welding/cutting results may seem to be a bizarre coincidence at first sight. However, results of this type are very natural in view of conjectures connecting LQG and random planar maps.

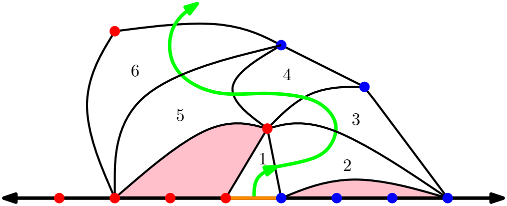

"Domain Markov half planar" map with marked boundary edge. Vertices to the left and right of edge colored red and blue. Percolation exploration from marked edge

- Left and right boundary lengths evolve independently and have independent increments
- Components cut off from infinity have i.i.d. structure

Our results in the continuum are analogies of these discrete observations

KPZ interpretation

Can give mathematical treatment of the heuristics used by Duplantier and others to predict quantum and Euclidean dimensions of random fractals.

KPZ interpretation

Can give mathematical treatment of the heuristics used by Duplantier and others to predict quantum and Euclidean dimensions of random fractals.

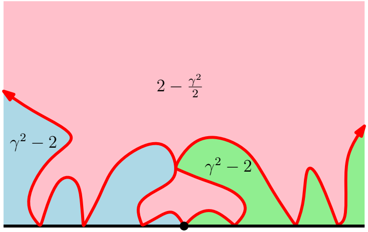

- Draw an $\mathrm{SLE}_{\kappa'}$ process, $\kappa' = \frac{16}{\gamma^2} \in (4, 8)$, η' on top of an independent $\frac{3\gamma^2}{2} - 2$ wedge

KPZ interpretation

Can give mathematical treatment of the heuristics used by Duplantier and others to predict quantum and Euclidean dimensions of random fractals.

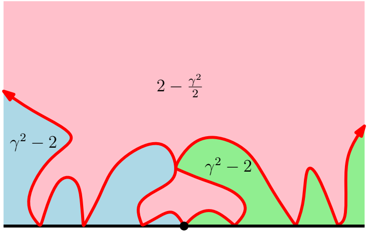

- Draw an $\mathrm{SLE}_{\kappa'}$ process, $\kappa' = \frac{16}{\gamma^2} \in (4, 8)$, η' on top of an independent $\frac{3\gamma^2}{2} - 2$ wedge
- Region between left and right boundaries of η' is a $2 - \frac{\gamma^2}{2}$ wedge

KPZ interpretation

Can give mathematical treatment of the heuristics used by Duplantier and others to predict quantum and Euclidean dimensions of random fractals.

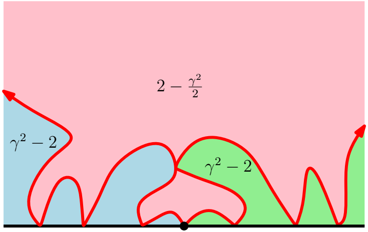

- Draw an $\mathrm{SLE}_{\kappa'}$ process, $\kappa' = \frac{16}{\gamma^2} \in (4, 8)$, η' on top of an independent $\frac{3\gamma^2}{2} - 2$ wedge
- Region between left and right boundaries of η' is a $2 - \frac{\gamma^2}{2}$ wedge
- Region to the left (resp. right) of left (resp. right) boundary is a $\gamma^2 - 2$ wedge

KPZ interpretation

Can give mathematical treatment of the heuristics used by Duplantier and others to predict quantum and Euclidean dimensions of random fractals.

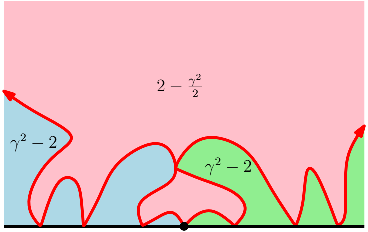

- Draw an $\mathrm{SLE}_{\kappa'}$ process, $\kappa' = \frac{16}{\gamma^2} \in (4,8)$, η' on top of an independent $\frac{3\gamma^2}{2} - 2$ wedge
- Region between left and right boundaries of η' is a $2 - \frac{\gamma^2}{2}$ wedge
- Region to the left (resp. right) of left (resp. right) boundary is a $\gamma^2 - 2$ wedge
- What does a "typical" $\mathrm{SLE}_{\kappa'}$ double point look like?

KPZ interpretation

Can give mathematical treatment of the heuristics used by Duplantier and others to predict quantum and Euclidean dimensions of random fractals.

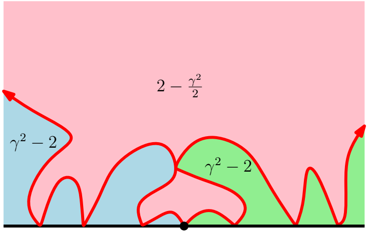

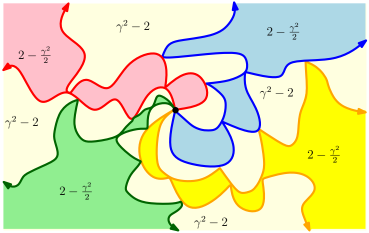

- Draw an $\mathrm{SLE}_{\kappa'}$ process, $\kappa' = \frac{16}{\gamma^2} \in (4,8)$, η' on top of an independent $\frac{3\gamma^2}{2} - 2$ wedge
- Region between left and right boundaries of η' is a $2 - \frac{\gamma^2}{2}$ wedge
- Region to the left (resp. right) of left (resp. right) boundary is a $\gamma^2 - 2$ wedge
- What does a "typical" $\mathrm{SLE}_{\kappa'}$ double point look like? Should have four $2 - \frac{\gamma^2}{2}$ wedges (the $\mathrm{SLE}_{\kappa'}$ strands) alternating with four $\gamma^2 - 2$ wedges (space in between)

KPZ interpretation

Can give mathematical treatment of the heuristics used by Duplantier and others to predict quantum and Euclidean dimensions of random fractals.

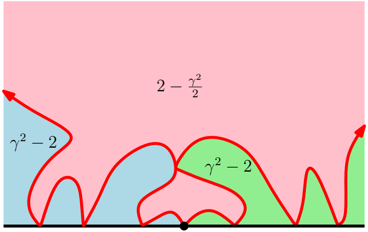

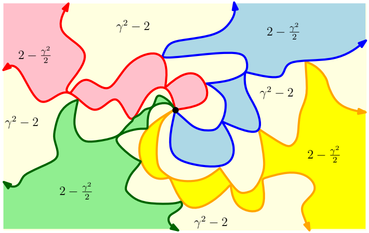

- Draw an $\mathrm{SLE}_{\kappa'}$ process, $\kappa' = \frac{16}{\gamma^2} \in (4,8)$, η' on top of an independent $\frac{3\gamma^2}{2} - 2$ wedge
- Region between left and right boundaries of η' is a $2 - \frac{\gamma^2}{2}$ wedge
- Region to the left (resp. right) of left (resp. right) boundary is a $\gamma^2 - 2$ wedge
- What does a "typical" $\mathrm{SLE}_{\kappa'}$ double point look like? Should have four $2 - \frac{\gamma^2}{2}$ wedges (the $\mathrm{SLE}_{\kappa'}$ strands) alternating with four $\gamma^2 - 2$ wedges (space in between)
- Cone weight $= 4(2 - \frac{\gamma^2}{2}) + 4(\gamma^2 - 2) = 2\gamma^2 \to (\frac{2}{\gamma} - \frac{\gamma}{2}) \log|\cdot|$ singularity

KPZ interpretation

Can give mathematical treatment of the heuristics used by Duplantier and others to predict quantum and Euclidean dimensions of random fractals.

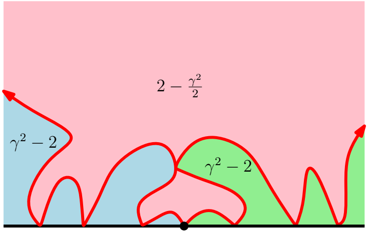

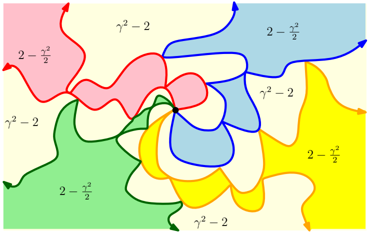

- Draw an $\mathrm{SLE}_{\kappa'}$ process, $\kappa' = \frac{16}{\gamma^2} \in (4,8)$, η' on top of an independent $\frac{3\gamma^2}{2} - 2$ wedge
- Region between left and right boundaries of η' is a $2 - \frac{\gamma^2}{2}$ wedge
- Region to the left (resp. right) of left (resp. right) boundary is a $\gamma^2 - 2$ wedge
- What does a "typical" $\mathrm{SLE}_{\kappa'}$ double point look like? Should have four $2 - \frac{\gamma^2}{2}$ wedges (the $\mathrm{SLE}_{\kappa'}$ strands) alternating with four $\gamma^2 - 2$ wedges (space in between)
- Cone weight $= 4(2 - \frac{\gamma^2}{2}) + 4(\gamma^2 - 2) = 2\gamma^2 \to (\frac{2}{\gamma} - \frac{\gamma}{2}) \log|\cdot|$ singularity
- Can deduce quantum scaling exponent; applying the KPZ formula gives Euclidean scaling exponent. Matches rigorously determined value by M., Wu.

Connection with Quantum Loewner Evolution

- Have described two senses in which one can try to show that FK weighted RPM converge to LQG:
  - Conformal embedding
  - Mating of trees

Connection with Quantum Loewner Evolution

- Have described two senses in which one can try to show that FK weighted RPM converge to LQG:
  - Conformal embedding
  - Mating of trees
- Also natural to show that FK weighted RPM converge to LQG as metric spaces

Connection with Quantum Loewner Evolution

- Have described two senses in which one can try to show that FK weighted RPM converge to LQG:
  - Conformal embedding
  - Mating of trees
- Also natural to show that FK weighted RPM converge to LQG as metric spaces
- So far, the metric space limit has only been constructed for uniform RPM ($q = 1$): the Brownian map

Connection with Quantum Loewner Evolution

- Have described two senses in which one can try to show that FK weighted RPM converge to LQG:
  - Conformal embedding
  - Mating of trees
- Also natural to show that FK weighted RPM converge to LQG as metric spaces
- So far, the metric space limit has only been constructed for uniform RPM ($q = 1$): the Brownian map
- We have constructed a new universal family of growth processes called QLE (candidate for the scaling limit of DLA, Eden model, and related models on RPM)

Connection with Quantum Loewner Evolution

- Have described two senses in which one can try to show that FK weighted RPM converge to LQG:
  - Conformal embedding
  - Mating of trees
- Also natural to show that FK weighted RPM converge to LQG as metric spaces
- So far, the metric space limit has only been constructed for uniform RPM ($q = 1$): the Brownian map
- We have constructed a new universal family of growth processes called QLE (candidate for the scaling limit of DLA, Eden model, and related models on RPM)
- We have also recently announced a program to show that $\mathrm{QLE}(8/3, 0)$ can be used to endow $\sqrt{8/3}$-LQG with a metric which is isometric to the Brownian map

Connection with Quantum Loewner Evolution

- Have described two senses in which one can try to show that FK weighted RPM converge to LQG:
  - Conformal embedding
  - Mating of trees
- Also natural to show that FK weighted RPM converge to LQG as metric spaces
- So far, the metric space limit has only been constructed for uniform RPM ($q = 1$): the Brownian map
- We have constructed a new universal family of growth processes called QLE (candidate for the scaling limit of DLA, Eden model, and related models on RPM)
- We have also recently announced a program to show that $\mathrm{QLE}(8/3, 0)$ can be used to endow $\sqrt{8/3}$-LQG with a metric which is isometric to the Brownian map
- Many steps of this program have already been carried out in the "mating of trees"

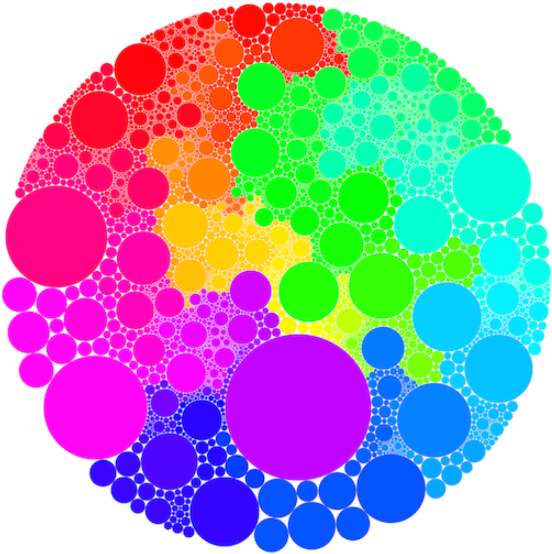

Thanks!